

## X-rays affect cytoskeleton assembly and nanoparticle uptake: Preliminary results

VALERIA PANZETTA<sup>(1)</sup>, MARIAGABRIELLA PUGLIESE<sup>(2)</sup>, GIOIA DI GENNARO<sup>(1)</sup>,  
COSTABILE FEDERICO<sup>(1)</sup>, CECILIA ARRICHELLO<sup>(3)</sup>, PAOLO MUTO<sup>(3)</sup>,  
PAOLO A. NETTI<sup>(1)(2)(3)(4)</sup> and SABATO FUSCO<sup>(1)</sup>

- <sup>(1)</sup> *Interdisciplinary Research Centre on Biomaterials (CRIB), Università degli Studi di Napoli "Federico II" - Piazzale Tecchio 80, 80125 Naples, Italy*
- <sup>(2)</sup> *Dipartimento di Fisica, Università degli Studi di Napoli "Federico II" and INFN, Sezione di Napoli - Monte S. Angelo, Via Cintia, 80126 Naples, Italy*
- <sup>(3)</sup> *Radiotherapy Unit, Istituto Nazionale Tumori-IRCCS-Fondazione "G. Pascale" Via Semmola, 53, 80131 Naples, Italy*
- <sup>(4)</sup> *Center for Advanced Biomaterials for Healthcare@CRIB, Istituto Italiano di Tecnologia (IIT) - Largo Barsanti e Matteucci 53, 80125 Naples, Italy*

received 4 December 2018

**Summary.** — Alterations of the cytoskeleton are commonly associated with tumor genesis and cancer progression. For this reason, the characterization of cytoskeleton-associated functions and properties is important to optimize the outcomes to classical and more recent therapeutic approaches, such as chemotherapy, radiotherapy and cancer nanomedicine. In such context, this work investigated the synergy between cancer nanomedicine and radiotherapy. In particular, the effects over time (24 and 48 h) of two different doses of X-rays (2 and 10 Gy) on spreading area, morphological parameters and the internalization mechanism of carboxylated nanoparticles in mammary epithelial cells and mammary adenocarcinoma cells were investigated.

### 1. – Introduction

The recent literature has demonstrated that the cytoskeleton (CSK) acts as an epigenetic determinant of several cell functions, such as adhesion, motility, proliferation, intracellular trafficking and differentiation [1]. Much attention has been paid to the role of the CSK in many diseases genesis and progression and, for example, it is now widely recognized that cancer and metastatic cells are generally softer than their healthy counterpart [2-4]. In this context, the characterization of CSK-associated functions and properties is important to develop alternative diagnostic tools able to understand the

response to classical and more recent therapeutic approaches, such as chemotherapy, radiotherapy and cancer nanomedicine, and, specifically, to optimize their outcomes also by their simultaneous combination.

In previous studies it has been observed that ionizing radiations can have appreciable effects both on the migration capability of cells and the structural properties of the CSK [5-9]. In particular, in some of the aforementioned works the authors found out that X-rays are able to induce a significant increase of adhesion and the consequent decrease of the migratory ability of transformed tumor-like fibroblasts.

Furthermore, it is now recognized the key role of nanomedicine in cancer treatment [10]. In fact, nanoparticles (NPs) can be used as vehicles for efficient anti-cancer drug delivery and, at the same time, recent investigations have also highlighted an active involvement of the CSK assembly in the mechanism of internalization of NPs [11, 12].

In such context, this work investigated the synergy between cancer nanomedicine and radiotherapy. In particular, the effects over time (24 and 48 h) of two different doses of X-rays (2 and 10 Gy) on spreading area, morphological parameters and the internalization mechanism of carboxyl-functionalized NPs (uptake) in mammary epithelial cells, MCF10A, and mammary adenocarcinoma cells, MCF7, were investigated.

## 2. – Materials and methods

**2.1. Cell cultures and X-ray irradiation.** – Experiments were performed on mammary epithelial cells, MCF10A, and mammary adenocarcinoma cells, MCF-7. MCF10A cells were grown in a nutrient-rich MEBM medium along with the additives obtained from Lonza/Clonetics Corporation as a kit (MEGM, Kit Catalog No. CC-3150) and MCF-7 cells in a EMEM medium supplemented with 10% fetal bovine serum (FBS), 1% penicillin/streptomycin and 1% L-glutamine at 37 °C with 5% CO<sub>2</sub>.

Cell lines were exposed to X-rays (photon beams) delivered by the LINAC SYNERGY AGILITY (ELEKTA) with field size (20 × 20) cm<sup>2</sup>, using the high endpoint energy of 6 MeV, at the National Cancer Institute “PASCALÉ” of Naples. The two cell lines were irradiated with two different doses of 2 Gy and 10 Gy.

**2.2. Cell proliferation.** – MCF10A and MCF7 cells were cultured at a concentration of 2000 cells/cm<sup>2</sup>. Cell proliferation was evaluated by image analysis. Cells were fixed with 4% paraformaldehyde for 20 min, stained with Hoechst 33342 (Sigma) at 72 h from irradiation. Samples were imaged using an inverted microscope system (Cell-R, Olympus, Japan) equipped with a 4× objective. Images of blue nuclei were captured from cell samples. Fluorescent images were imported into ImageJ software (NIH, USA) for post-processing and analysis. Images were converted to grayscale (8-bit or 16-bit grayscale) and then to binary images by using manual thresholding. The menu command “Analyze particle” was used to count the cell number in each image.

**2.3. Cell spreading.** – MCF10A and MCF7 cells were cultured at a density of 2000 cells/cm<sup>2</sup>, respectively. Cells were fixed with 4% paraformaldehyde for 20 min, stained with Alexa 568-phalloidin to quantify the spreading area in control condition and at 24 and 72 h from irradiation.

**2.4. Quantification of NP cellular uptake.** – Cells were incubated with red NPs at the final concentration of  $3.6 \times 10^9$  NPs mL<sup>-1</sup> for 1 h and 6 h. After incubation, cells were rinsed five times with PBS to remove non-internalized nanoparticles, fixed with 4% paraformaldehyde for 20 min, and the cells were stained with Alexa 488-phalloidin

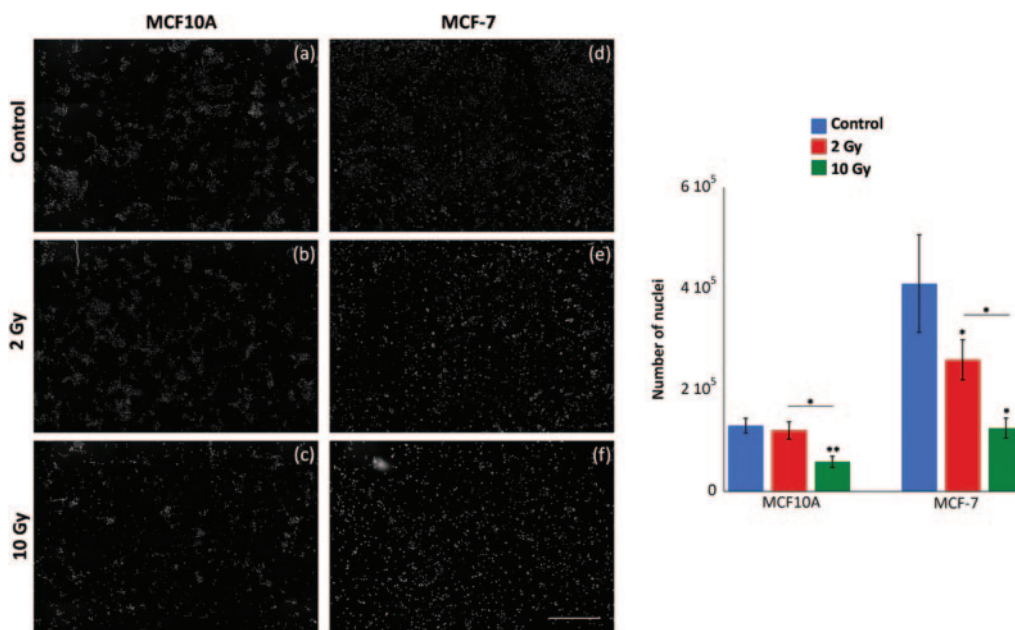


Fig. 1. – Nuclei were counterstained with Hoechst 33342 and counted in 6 images for each cell line and each condition. The data of proliferation are presented as mean  $\pm$  SEM. \*:  $P < 0.05$ ; \*\*:  $P < 0.01$ . Scale bar, 1 mm.

(Molecular Probes). Z-sectioning images of cells incubated with fluorescent NPs were collected with a confocal laser scanning microscope (Zeiss LSM 710) equipped with an argon and He–Ne laser lines at the wavelengths of 488 nm and 543 nm, respectively, using a 40 $\times$  oil immersion objective (NA 1.30). The pinhole size was 90  $\mu$ m and Z-stacks spaced by 0.5  $\mu$ m covering the total cell volume were recorded. The images resolution was fixed at 2048  $\times$  2048 squared pixels (0.05  $\mu$ m/px). The image analysis of fluorescent NPs internalized by cells was performed by NIH software (Fiji ImageJ). Briefly, a maximum projection image for both color channels was constructed from the consecutive focal planes. Green images were used to extract individual cell outlines using ImageJ ROI manager tool and COOH-NP internalization at each time-point was evaluated in terms of integrated fluorescence intensity of NPs within individual cell boundaries.

### 3. – Results

**3.1. The effects of X-rays on cell proliferation.** – In order to evaluate the MCF10A and MCF-7 reproductive activity, cells were plated at equal densities and recounted 72 h after irradiation. In control condition, MCF10A cells showed a significantly reduced proliferation activity in comparison with MCF7 cells. In fact, after 72 h the number of cells increased by 6 and 20 times for MCF10A and MCF-7, respectively. Furthermore, the results showed that only 10 Gy delivered dose inhibited the growth and the proliferation of MCF10A, while MCF-7 proliferation ability was markedly reduced by both X-rays doses (fig. 1). In particular, the MCF10A growth was halved after irradiation with 10 Gy

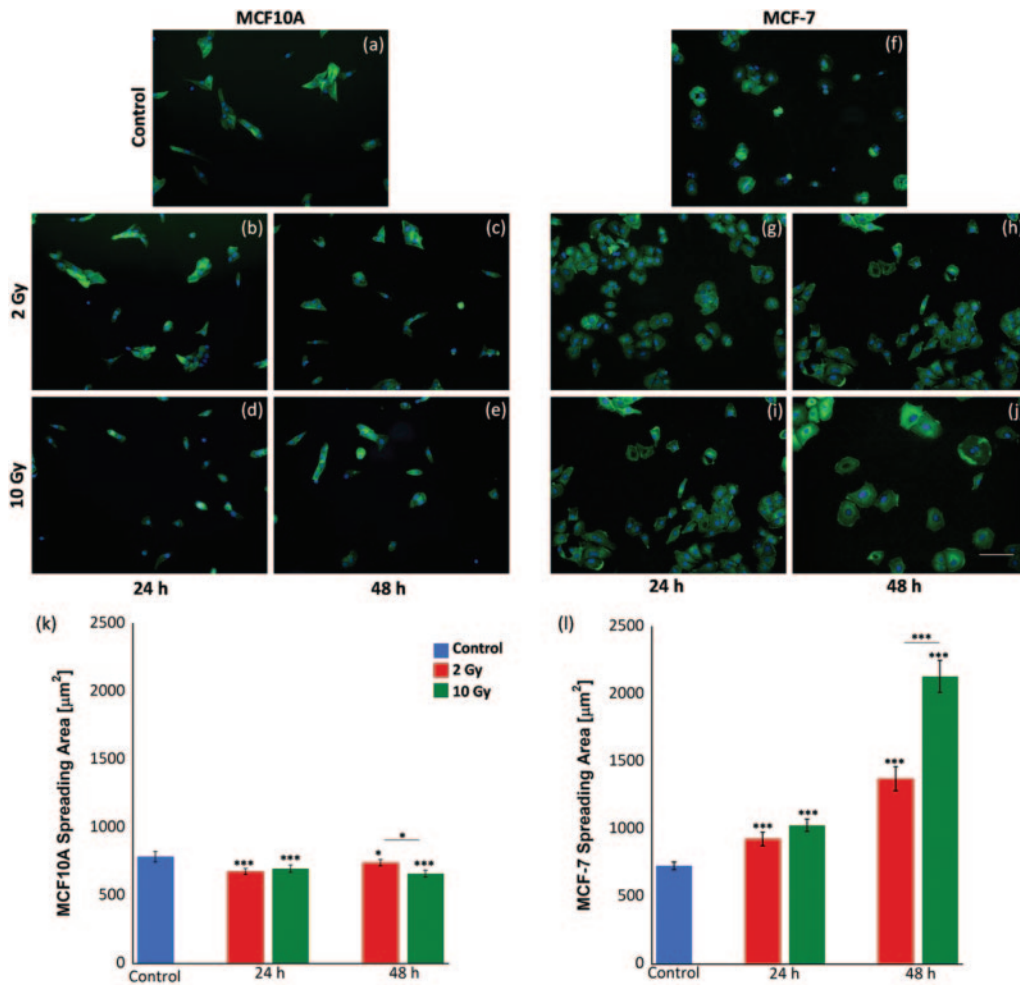


Fig. 2. – The morphology and cytoskeleton in MCF10A and MCF-7 cells are compared before ((a),(f)) and after X-irradiation with doses of 2 Gy ((b),(c),(g),(h)) and 10 Gy ((d),(e),(i),(j)). The spreading area data are presented as mean  $\pm$  SEM. \*:  $P < 0.05$ ; \*\*\*:  $P < 0.001$ . Scale bar, 100  $\mu\text{m}$ .

doses, while MCF-7 proliferation was reduced by 40% and 70%, when irradiated with doses of 2 and 10 Gy, compared to control cells.

**3.2. The effects of X-rays on cell adhesion.** – The morphology and the cytoskeleton in MCF10A and MCF-7 cells are compared in fig. 2(a)–(j). In control conditions, the cellular shape of MCF10A cells appeared quite elongated and completely flattened, while MCF-7 cells showed a polygonal cell shape (fig. 2(a) and (f)). Both cell lines tend to grow attached to the plastic plates in discrete patches, even if cultured at low density. In addition, in MCF10A cells actin stress fibers were evident throughout the cell body and the perinuclear actin cap, wrapping the nucleus, was observable. In MCF-7 cells it is possible to observe cortical actin stress fibers around the cell boundary. These differences in the morphology and cytoskeleton structure reflected in the spreading area

which appeared slightly higher in MCF10A ( $847 \mu\text{m}^2$ ) than in MCF-7 cells ( $729 \mu\text{m}^2$ ). Twenty-four hours after irradiation, MCF10A and MCF7 resulted to be, respectively, less and more spread compared to control cells when irradiated (fig. 2(a),(b),(d),(f),(g),(i)). The effect seems to be maintained at 48 h for both cell lines and reinforced for tumor cells, which responded at X-irradiation in a dose-dependent manner (fig. 2(a),(c),(e)–(f),(h),(j)). Cells irradiated by X-rays presented actin filament accumulation, which, in turn, promotes a more flattened and spread morphology in the case of MCF-7 cells. The increase of tumor cell spreading at values significantly greater than those of normal cells in control condition could be explained by considering that MCF-7 cells are characterized by a cell volume remarkably higher than MCF10A cells [13]

**3.3. The effects of X-rays on the NPs uptake.** – To investigate the effects of X-rays on the carboxyl-functionalized NPs uptake, cells were incubated with NPs at  $37^\circ\text{C}$  and two time points (1 and 6 h) in control conditions and after 24 and 48 h from irradiation. In particular, in MCF10A cells the image analysis showed that the NPs uptake was significantly higher in healthy cells than in tumor counterparts, probably because of the greater structuration of the CSK of MCF10A cells. As reported in fig. 3, the X-irradiation played a key role also in the internalization of NPs. Twenty-four hours after irradiation, COOH-NPs uptake at 1 h was impaired in MCF10A cells as a consequence of their reduced adhesion, while the ability to internalize the NPs was not significantly changed at 6 h. Over longer periods (48 h) the effect of the low dose was reduced and the nanoparticles uptake did not result significantly decreased in irradiated cells. On the other hand, the cells irradiated with a dose of 10 Gy continued to internalize a lower amount of NPs at 48 h, as a consequence of the more persistent effect of X-rays also on the adhesiveness of MCF10A cells. On the contrary, the increased adhesion and the more structured CSK of MCF7 cells after irradiation enhanced significantly the internalization of NPs in tumor cells already at 24 h. This outcome was strengthened at 48 h in a dose-dependent way.

#### 4. – Discussion

Cancer onset, progression and aggression are deeply associated to changes in the cytoskeletal structure, cellular shape, differentiation, proliferation, adhesion, and migration [1-4, 14]. These alterations are responsible of the decreased stiffness of cancer cells and the extent of the cell compliance correlates with aggressiveness and metastatic potential of cancer cells [2, 3, 8]. The knowledge of the physical properties of tumor cells and their microenvironment is fundamental to understand the molecular pathways which drive the cell transformation and cancer progression, but also to develop effective therapeutics to treat cancer and to verify their effectiveness. In this work we have evaluated the effects over time (24 and 48 h) of two different doses of X-rays (2 and 10 Gy) on the adhesiveness and cytoskeleton structure of mammary epithelial cells (MCF10A) and mammary adenocarcinoma cells (MCF-7). As already observed in previous works, radiations had important consequences on the cell adhesiveness, evaluated by measuring the cell spreading area. Indeed, healthy cells reduced their spreading area already at 24 h and this effect was partially recovered at 48 h for the low dose and slightly reinforced for the high one. On the contrary, irradiated tumor cells showed a more spread area than control cells already at 24 h and the increase of adhesiveness was also confirmed by the augmentation of stress fibers consequent to the irradiation. Over longer periods, the spreading area of MCF-7 cells was further increased in a dose-dependent manner.

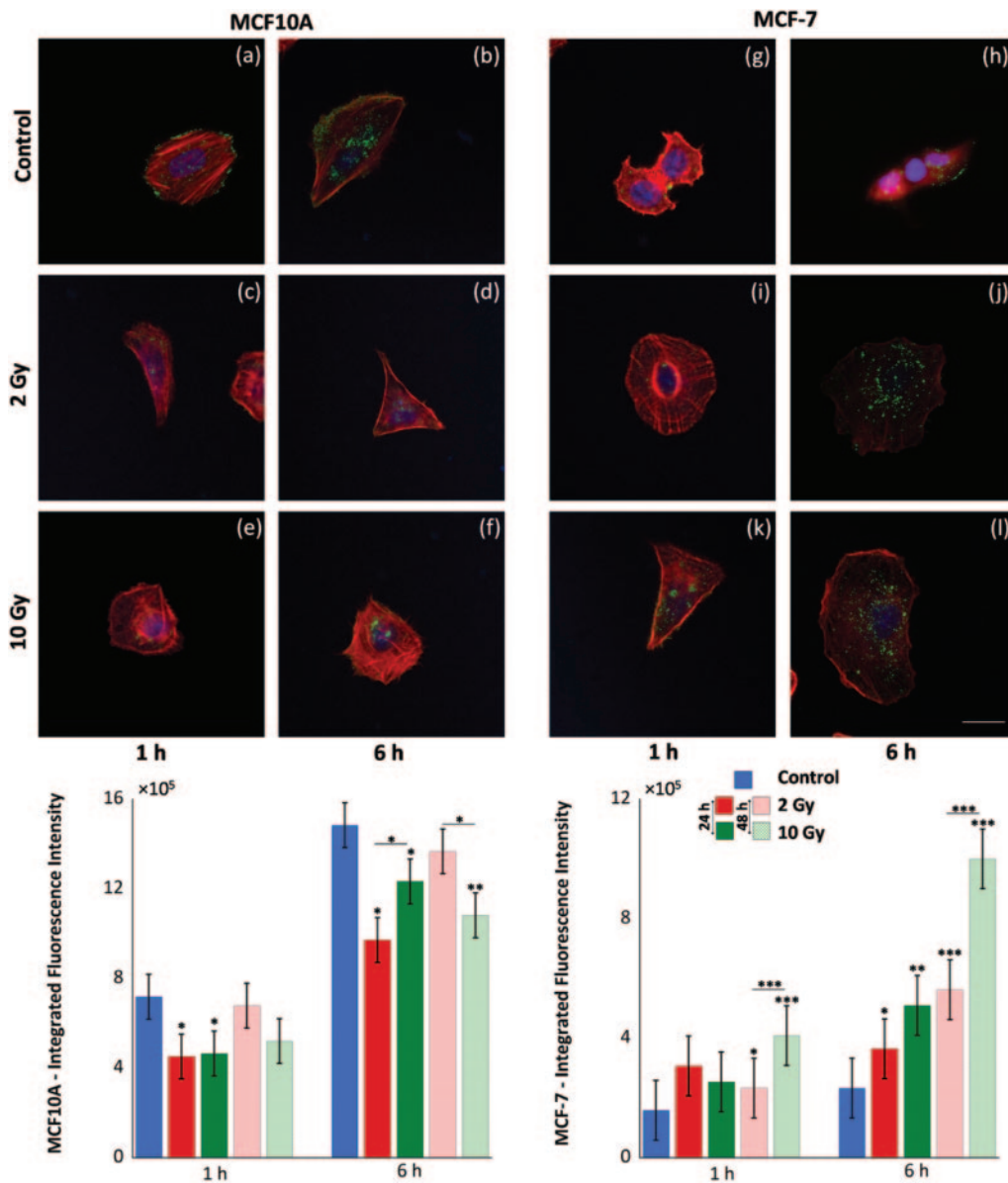


Fig. 3. – MCF10A and MCF-7 cells were incubated with COOH-NPs for 1 and 6 h after 24 and 48 h from irradiation. The NPs uptake was found to be affected by X-rays in an opposite way in MCF10A and MCF-7 cells. The NPs uptake was evaluated in terms of integrated fluorescence intensity and the data are presented as mean  $\pm$  SEM. \*:  $P < 0.05$ ; \*\*:  $P < 0.01$ ; \*\*\*:  $P < 0.001$ . Scale bar, 20  $\mu$ m.

It is interesting to highlight the opposite behaviour of the two cell lines and the ability of normal cells to partially recover their initial physical properties (both average and  $p$ -value of spreading increased passing from 24 to 48 h) at least when low doses were administered. The consequences of the increased adhesion of irradiated tumor cells are

controversial. Indeed, some works report an increased cell adhesion together with increased motility and invasiveness of surviving cancer cells [15]. Nevertheless, we have previously observed that in normal and transformed fibroblasts the growth of the cell spreading area was associated to the stiffening of the CSK, to the enhanced expression of adhesive surface molecules and, in particular, to the reduced motility of both cell lines [7-9]. Anyway, the cell's intrinsic response to ionizing radiations can be used to improve the efficiency of classical and more recent therapeutic approaches, such as chemotherapy and cancer nanomedicine, when they are used in combination with radiotherapy. In particular, nanomedicine is running fast in developing new and promising tumor-targeted drug delivery systems which are able to enhance antitumor efficacy and to attenuate drug toxicity. For these reasons, the effects of X-rays on the internalization mechanism of carboxyl-functionalized NPs with diameters of 100 nm were analyzed and explained by taking into consideration the pivotal role of the cell cytoskeleton. The COOH-NPs uptake was incubated with both cell lines in control conditions and after irradiation and, assuming that the fluorescence intensity is proportional to the number of internalized NPs, the fluorescence within individual cells was used as a parameter to evaluate the efficiency of cellular uptake. Compared to tumor cells, MCF10A cells internalized NPs in a greater amount both at 1 and 6 h as a consequence of the more structured actin of CSK. Indeed, as previously reported, there exists a positive correlation between cell adhesion and NPs uptake which depends on the direct involvement of CSK in endocytic pathways [11]. Similarly, the changes in the spreading area and in the structure of the CSK, found here for normal and tumor cells after irradiation, affected the amount of internalized NPs. Indeed, the uptake process resulted to be significantly impaired in MCF10A cells and, as observed for the spreading area, this effect persisted for the dose of 10 Gy, while a partial recovery was measured for the low dose. On the contrary, it has been observed that the radiations significantly increase the NPs uptake in tumor cells, particularly at 48 h from irradiation, activating an internalization pathway directly correlated to the dynamics of the CSK. In fact, as ascertained, X-rays induce in MCF-7 cells structural variations of CSK, which resulted in increased adhesiveness and augmented CSK structuration. The formation of a more structured CSK after X-irradiation, in turn, promotes the internalization of NPs in a larger amount. It is necessary to underline that the NPs used in this work were free of surface conjugation with specific ligand molecules. Then, in the future, NPs able to activate a tumor specific pathway directly involving the cytoskeleton could be designed and fabricated. Further and more detailed studies on the effects of X-rays on the expression of adhesion and signaling molecules strictly related to the CSK, such as integrins, could provide new insights into the design of promising ligand-based targeting approaches. Finally, these findings can give fundamental information for the development of new strategies for combinations and timings of radiotherapy and cancer nanomedicine.

## 5. – Conclusions

In conclusion, it was found that X-rays increased significantly tumor cell adhesiveness, evaluated by spreading area, CSK structure and COOH-NPs uptake. On the contrary, ionizing radiations reduced the cell spreading area and NPs uptake of normal cells, even if these effects resulted to be less persistent in MCF10A cells when the low dose was used. Future studies could give a deeper comprehension of the role of cytoskeletal and surface adhesive molecules involved in these processes. More importantly, this knowledge could

be used for the development of new drug-radiotherapy combinations and for the design of specific ligand-targeted nanocarriers.

## REFERENCES

- [1] PEYTON S. R. *et al.*, *Cell Biochem. Biophys.*, **47** (2007) 300.
- [2] GUCK J. *et al.*, *Biophys. J.*, **88** (2005) 2689.
- [3] CROSS S. E. *et al.*, *Nanotechnol.*, **19** (2008) 384003.
- [4] PANZETTA V. *et al.*, *Acta Biomater.*, **57** (2017) 34.
- [5] WOLOSCHAK G. E. *et al.*, *Mol. Carcinog.*, **3** (1990) 374.
- [6] MONCHARMONT C. *et al.*, *Crit. Rev. Oncol. Hematol.*, **92** (2014) 133.
- [7] PANZETTA V. *et al.*, *J. Mech. Med. Biol.*, **15** (2015) 1540022.
- [8] PANZETTA V. *et al.*, *Cytoskeleton*, **74** (2017) 40.
- [9] PANZETTA V. *et al.*, *ENBENG 2017 - IEEE 5th Portuguese Meeting on Bioengineering, Proceedings*, Vol. **16** (2017) p. 7889448.
- [10] KIM W. *et al.*, *J. Control. Release*, **200** (2015) 138.
- [11] PANZETTA V. *et al.*, *ACS Biomater. Sci. Eng.*, **3** (2017) 1586.
- [12] HE L. *et al.*, *Sci. Rep.*, **8** (2018) 7318.
- [13] GELTMEIER A. *et al.*, *PLoS ONE*, **10** (2015) e0134999.
- [14] BOSCH-FORTEA M. *et al.*, *Curr. Opin. Cell Biol.*, **50** (2018) 42.
- [15] TSUTSUMI K. *et al.*, *Cell Struct. Funct.*, **34** (2009) 89.